Stem Cell Reports
Article
OPEN ACCESS

Comparative miRNA-Based Fingerprinting Reveals Biological Differences in Human Olfactory Mucosa- and Bone-Marrow-Derived Mesenchymal Stromal Cells

Susan Louise Lindsay,[1] Steven Andrew Johnstone,[1] Michael Anthony McGrath,[1] David Mallinson,[1,2] and Susan Carol Barnett[1,*]

[1]Institute of Infection, Inflammation and Immunity, Glasgow Biomedical Research Centre, University of Glasgow, Sir Graeme Davies Building, 120 University Place, Glasgow G12 8TA, UK
[2]Sistemic UK, Kelvin Campus, Maryhill Road, Glasgow G20 0SP, UK
*Correspondence: susan.barnett@glasgow.ac.uk
http://dx.doi.org/10.1016/j.stemcr.2016.03.009

SUMMARY

Previously we reported that nestin-positive human mesenchymal stromal cells (MSCs) derived from the olfactory mucosa (OM) enhanced CNS myelination in vitro to a greater extent than bone-marrow-derived MSCs (BM-MSCs). miRNA-based fingerprinting revealed the two MSCs were 64% homologous, with 26 miRNAs differentially expressed. We focused on miR-146a-5p and miR-140-5p due to their reported role in the regulation of chemokine production and myelination. The lower expression of miR-140-5p in OM-MSCs correlated with higher secretion of CXCL12 compared with BM-MSCs. Addition of CXCL12 and its pharmacological inhibitors to neural co-cultures supported these data. Studies on related miR-146a-5p targets demonstrated that OM-MSCs had lower levels of Toll-like receptors and secreted less pro-inflammatory cytokines, IL-6, IL-8, and CCL2. OM-MSCs polarized microglia to an anti-inflammatory phenotype, illustrating potential differences in their inflammatory response. Nestin-positive OM-MSCs could therefore offer a cell transplantation alternative for CNS repair, should these biological behaviors be translated in vivo.

INTRODUCTION

Bone-marrow-derived mesenchymal stromal cells (BM-MSCs) have been reported to secrete neurotrophic cytokines as well as a range of pro-inflammatory cytokines, chemokines, and other soluble growth factors (Nakano et al., 2010; Ma et al., 2013). Because of these properties, their feasibility and safety of administration were assessed in clinical trials for the treatment of multiple sclerosis (MS), with results suggesting they can modulate the immune response, protect neurons from degeneration, and improve disease progression (Bonab et al., 2012; Connick et al., 2012). MSCs have been isolated from a range of tissues including bone marrow, adipose, pancreas, skin, muscle, tendon, umbilical cord, skin, and dental pulp (Hass et al., 2011; Wang et al., 2013). We have recently isolated MSCs from the lamina propria of human olfactory mucosa (OM) (termed OM-MSCs; Lindsay et al., 2013); a tissue of fundamental interest in the context of neuroprotection and repair because of its ability to continually support neurogenesis throughout life (Graziadei and Monti Graziadei, 1985). Our previous studies have demonstrated that OM-MSCs have a similar antigenic profile and differentiation properties to BM-MSCs (Lindsay et al., 2013). However, the entire OM-MSC population expressed nestin, while conversely around 50% of BM-MSCs were nestin-positive, despite being isolated using identical methodology (Johnstone et al., 2015). Importantly, there was a major difference in the ability of OM-MSCs to promote CNS myelination in vitro via a secreted factor(s) (Lindsay et al., 2013).

Since these properties can be explained by a vast number of genes, we decided to use a microRNA (miRNA) array approach to identify differences and similarities between the two MSCs. miRNAs are an abundantly expressed family of small post-transcriptional regulators (18–24 nucleotides). They control gene expression by modulating the translation (usually by repression), stability, and localization of specific mRNA targets (Ambros, 2001). They regulate numerous functions ranging from cell differentiation, proliferation, and apoptosis to fat metabolism (Skalnikova et al., 2011). miRNAs are thought to act as regulatory signals for maintaining stemness, self-renewal, and differentiation in adult stem cells and are therefore important in controlling classic stem cell properties (Collino et al., 2011; Tomé et al., 2011). Characterization of miRNAs from MSCs of different tissue sources could be relevant not only as a marker of the cell but also to fully understand their biological activities and give an insight into what makes them different (Collino et al., 2011). Recent work has described nestin-positive MSCs as a subpopulation (Tondreau et al., 2004; Wiese et al., 2004) that originates not from the mesoderm but from the neural crest giving nestin-positive MSCs specialized niche functions over nestin-negative MSCs (Isern and Méndez-Ferrer, 2011; Isern et al., 2014). Therefore, in this investigation, we have compared the miRNA profile of nestin-positive OM-MSCs with classical BM-MSCs to determine any important

biological differences that, in particular, may be relevant to their role in cell transplantation therapies for the treatment of demyelinating conditions, such as MS.

RESULTS

miRNA Analysis of OM-MSCs and BM-MSCs

Analysis revealed 195 mature miRNAs detected in OM-MSCs (n = 4 patient samples) and BM-MSCs (n = 4 patient samples), of which 125 were equivalently expressed (EE). This demonstrates 64% identity, despite being isolated from different tissues; moreover, 27 of these EE miRNAs have already been reported for BM-MSCs (Gao et al., 2011; Figure 1A). These data suggest that MSCs derived from OM express a similar core set of miRNAs compared with BM.

In contrast, 26 were differentially expressed (DE) across all samples, with 16 being downregulated in OM-relative to BM-MSCs (Figure 1B). These miRNAs have over 300 targets, therefore a contextual approach was adopted whereby miRNAs associated with MSC biology were identified. Since our previous comparative studies identified differences in cell proliferation, cell survival, and myelination (Lindsay et al., 2013), we focused on miR-140-5p and miR-146a-5p (Figure 1B), which have already been identified as key regulators of these processes (Suzuki et al., 2010; Göttle et al., 2010).

qPCR Analysis for miR-140-5p and miR-146a-5p

qPCR confirmed a significant 3.01-fold higher expression of miR-140-5p in BM-MSCs compared with OM-MSCs (n = 4 patient samples for both, $p < 0.05$; Figures 1C and 1E), and a significant 7.99-fold higher expression of miR-146a-5p in OM-compared with BM-MSCs (n = 4 patient samples for both, $p < 0.05$; Figures 1D and 1E), confirming the miRNA analysis.

Cytokine/Chemokine Analysis

GeneGo MetaCore analysis revealing high-confidence mRNA targets for miR-140-5p suggested SDF-1 (referred to as CXCL12 hereafter) secretion may be differentially regulated between the MSCs. Multiplex analysis of the conditioned media (CM) collected from OM- and BM-MSCs was performed with fibroblast (FB) and CD271-FT-CM used as comparisons (CM derived from n = 4 patient samples). Since we have previously shown that both FB-CM and CD271-FT-CM do not promote myelination (Lindsay et al., 2013), these were considered an appropriate comparison to ensure secreted factors were specifically generated from OM-MSCs (see Table 1); 13 were not detected and nine were secreted to equivalent levels across all groups (CCL1, CCL2, CCL3, CCL8, CX3CL1, G-CSF, CXCL10, SCF, and VEGF). CCL11 was significantly higher within both OM-MSC-CM and CD271-FT-CM compared with BM-MSC-CM and FB-CM ($p < 0.05$, all comparisons), suggesting the expression of a tissue-specific chemokine rather than MSC specific. CCL13 was significantly lower within FB-CM compared with all other cell type CM ($p < 0.05$, all comparisons), however, it was equivalently expressed within OM-MSCs, BM-MSCs, and CD271-FT-CM. CCL5 was markedly increased in CD271-FT-CM ($p < 0.01$). CXCL12 was the only cytokine present in significantly greater quantities in OM-MSC-CM compared with either BM-MSC-CM ($p < 0.01$), CD271-FT-CM ($p < 0.01$), or FB-CM ($p < 0.05$, Figure 2A). In addition, the neurotrophic factors BDNF, NT3, NT4/5, and NGF were assayed in BM- and OM-MSC-CM (n = 3 patient samples for both). NT3 was undetectable, and both cell types secreted equivalent low levels of BDNF (OM-MSC-CM, 19.2 ± 5.3 pg/ml; BM-MSC-CM, 11.9 ± 4.83 pg/ml) and NT4/5 (OM-MSC-CM, 21.9 ± 0.3 pg/ml; BM-MSC-CM, 20.0 ± 0.7 pg/ml). OM-MSC-CM contained significantly higher levels of NGF (33.8 ± 6.8 pg/ml) compared with BM-MSC-CM (1.2 ± 0.6 pg/ml).

Transfection of Cells with miR-140-5p Inhibitor and Mimic Affects Production of CXCL12 mRNA

OM- and BM-MSCs (n = 3, patient samples for both) were transfected with miR-140-5p antagomir or mimic, a random sequence miRNA molecule (scrambled control) or dH_2O (Figures 2B and 2C) to confirm their ability to modulate miR-140-5p expression. MiR-140-5p antagomir silenced expression, while the mimic significantly upregulated miR-140-5p in both OM- and BM-MSCs. These data confirm that levels of miR-140-5p can be modulated by both the antagomir and mimic.

To validate direct correlation of miR-140-5p and *CXCL12* expression, both MSC types were transfected with the miR-140-5p antagomir or mimic, and *CXCL12* mRNA levels were quantified (Figures 2D and 2E). The mimic resulted in virtually undetectable levels of *CXCL12* in both MSC types. Antagomir induced a significant increase in BM-MSCs compared with control levels ($p < 0.05$; Figure 2E), and although the levels of *CXCL12* mRNA were increased in OM-MSCs compared with the mimic, they were still below that of control OM-MSCs (Figure 2D), which inherently expressed higher levels of *CXCL12* mRNA than BM-MSCs. This confirms that increased levels of miR-140-5p negatively regulate the expression of *CXCL12*.

CXCL12 Promotes In Vitro CNS Myelination Which Is Inhibited Using the Neutralizing Antibody and Receptor Blocker to CXCL12

Our previous data suggest that OM-MSCs promoted in vitro CNS myelination via a secreted factor. Here

A

miRNAs	P_{FDR}	miRNAs	P_{FDR}
hsa-miR-21-5p	0.0080	hsa-miR-107	0.0130
hsa-miR-23a-3p	0.0200	hsa-miR-193b-3p	0.0080
hsa-miR-125b-5p	0.0290	hsa-miR-26a-5p	0.0080
hsa-miR-29a-3p	0.0100	hsa-miR-222-3p	0.0200
hsa-miR-100-5p	0.0240	hsa-miR-193a-3p	0.0130
hsa-miR-22-3p	0.0230	hsa-miR-210	0.0480
hsa-miR-27a-3p	0.0240	hsa-miR-99a-5p	0.0410
hsa-miR-199a-3p	0.0120	hsa-miR-214-3p	0.0230
hsa-miR-221-3p	0.0080	hsa-miR-125a-5p	0.0010
hsa-miR-16-5p	0.0240	hsa-miR-181a-5p	0.0490
hsa-miR-23b-3p	0.0080	hsa-miR-320a	0.0070
hsa-miR-130a-3p	0.0300	hsa-let-7e-5p	0.0420
hsa-miR-27b-3p	0.0040	hsa-miR-30d-5p	0.0230
hsa-miR-24-3p	0.0028		

B

miRNAs	P_{FDR}	FC	miRNAs	P_{FDR}	FC
hsa-miR-10b-5p	0.0012	8.5189	**hsa-miR-140-5p**	**0.0151**	**1.8377**
hsa-miR-335-5p	0.0405	4.2807	hsa-miR-140-3p	0.0216	1.6697
hsa-miR-3665	0.0304	4.2122	hsa-miR-1225-5p	0.0405	1.5027
hsa-miR-3188	0.0110	4.0233	hsa-miR-429	0.0405	-1.5192
hsa-miR-2861	0.0405	3.3465	hsa-miR-20a-5p	0.0405	-1.7979
hsa-miR-4281	0.0402	3.0499	hsa-miR-25-3p	0.0405	-1.798
hsa-miR-762	0.0405	2.9282	hsa-miR-106b-5p	0.0216	-1.8071
hsa-miR-874	0.0405	2.9067	hsa-miR-301a-3p	0.0304	-1.86
hsa-miR-1915	0.0365	2.8280	hsa-miR-195-5p	0.0304	-2.057
hsa-miR-638	0.0304	2.5847	hsa-miR-497-5p	0.0405	-2.0666
hsa-miR-424-5p	0.0405	2.4546	hsa-miR-93-5p	0.0365	-2.3525
hsa-miR-224-5p	0.0365	1.7639	hsa-miR-3529-3p	0.0405	-3.0606
hsa-miR-939	0.0304	1.5646	**hsa-miR-146a-5p**	**0.0405**	**-15.2891**

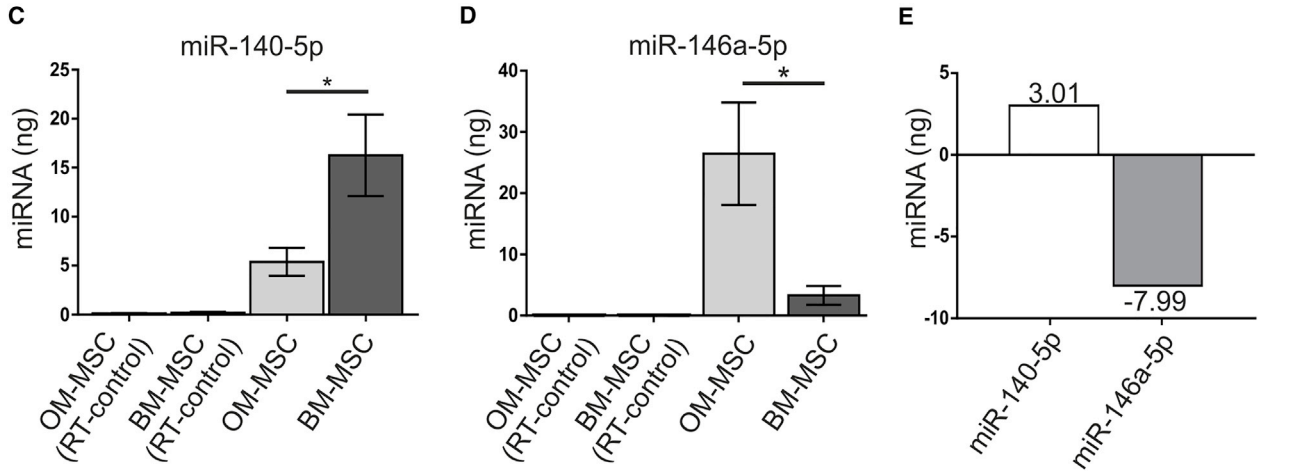

Figure 1. miRNA Profiling of OM-MSCs and BM-MSCs

(A) Twenty-seven equivocally expressed (EE) miRNAs in OM-MSCs (n = 4 patient samples) and BM-MSCs (n = 4 patient samples) that associate specifically with MSCs (significance determined at $P_{FDR} < 0.05$ rejects the null hypothesis and concludes that they are EE).

(B) Twenty-six differentially expressed (DE) miRNAs between both cell types. Table shows the fold change (FC) in expression of BM-MSCs versus OM-MSCs (n = 4 patient samples, significance at $P_{FDR} < 0.05$ and an FC $\geq$ 1.5). Two miRNAs of interest, hsa-miR-140-5p and hsa-miR-146a-5p, are highlighted in red.

(C) qPCR confirms miR-140-5p is significantly upregulated in BM-MSCs compared with OM-MSCs (n = 4 patient samples, mean ± SEM, *p < 0.05 determined by one-way ANOVA, Tukey's multiple comparison).

(D) qPCR confirms miR-146-5p is upregulated in OM-MSCs compared with BM-MSCs (n = 4 patient samples, mean ± SEM, *p < 0.05, determined by one-way ANOVA, Tukey's multiple comparison).

(E) FC in expression of miR-140-5p and miR-146-5p in OM-MSCs versus BM-MSCs.

we provide evidence that CXCL12 could be this factor. Myelinating CNS co-cultures were treated with CXCL12 (100 ng/ml), CXCL12 receptor CXCR4 blocker (AMD3100), OM-MSC-CM, as well as OM-MSC-CM treated with a neutralizing antibody to CXCL12 or AMD3100 (n = 4, all treatments and four different patient samples; Figures 3A and 3B). Media containing the CXCL12 neutralizing antibody or AMD3100 were used as controls. Exogenous CXCL12 significantly increased myelination almost 2-fold compared with controls ($p < 0.05$), which was blocked by AMD3100. The pro-myelinating effect of OM-MSC-CM ($p < 0.05$) was also reduced by AMD3100 and when treated with the neutralizing antibody to CXCL12. These data indicate that CXCL12 is at least partially responsible for the pro-myelinating effect of OM-MSCs.

Table 1. Multiplex Chemokine Analysis of CM Showing the Comparative Differences in Secreted Cytokines

Cytokine	Significant Difference
CXCL12	**<OM only
CCL1	NS
CCL2	NS
CCL3	NS
CCL8	NS
CX3CL1	NS
G-CSF	NS
CXCL10	NS
SCF	NS
VEGF	NS
CCL11	*<OM *<CD271-FT
CCL13	*>FB
CCL5	**<CD271-FT

NS, not significantly different; *<OM, *<CD271-FT, represents that the cytokine was secreted in significantly higher amounts in CM from OM-MSCs and CD271-FTl *>FB, represents it was present in significantly less amounts in fibroblasts (FB), **<CD271-FT or significantly higher in CD271-FT-CM. CXCL12 was the only chemokine secreted at significantly higher amounts in OM-MSC-CM compared with all other cell types (*$p < 0.05$, **$p < 0.01$, $n = 3$ for all, as determined by one-way ANOVA, Tukey's multiple comparison).

Transfection with miR-140-5p Antagomir or Mimic Can Affect In Vitro CNS Myelination

We next determined if modulating miR-140-5p in OM- or BM-MSCs can affect myelination in vitro. BM-MSC-CM was collected from cells transfected with the miR-140-5p antagomir and added to cultures (n = 6 patient samples; Figures 3C and 3D). Antagomir-transfected BM-MSC-CM significantly increased myelination by 1.64 ± 0.19-fold compared with control (n = 6 patient samples, $p < 0.05$) or that induced by control transfections (n = 6 patient samples, $p < 0.01$ for both). The increased myelination was brought back to levels that were not significant from control by the addition of either the antibody to CXCL12 or AMD3100 (n = 3 patient samples for both). CM derived from BM-MSCs transfected with miR-140-5p mimic (n = 3 patient samples) showed no increase in myelination from control. OM-MSC-CM collected from cells treated with miR-140-5p antagomir increased myelination compared with controls ($p < 0.05$) but was not significantly different to that produced by control transfections (n = 6, patient samples; Figures 3C and 3E). The pro-myelinating effect of CM collected from antagomir-treated OM-MSCs could be reduced in the presence of either the antibody to CXCL12 or AMD3100 (n = 3 patient samples for both). OM-MSC-CM collected from miR-140-5p mimic-treated cells reduced myelination to control. This confirms that miR-140-5p can induce OM- and BM-MSCs to increase CXCL12 secretion, which is pro-myelinating, since blocking its activity abolishes the effect.

CXCR4 Expression on Oligodendrocyte Precursor Cells and Microglia

CXCL12 is known to mediate its effect via CXCR4 and CXCR7, therefore cellular expression may help determine the mode of action. Oligodendrocyte precursor cells (OPCs) and microglia were both found to express CXCR4, however no expression was found on astrocytes (n = 3, all cell types; Figures 4A and 4B). Western blotting of CXCR4 revealed OPCs (n = 6) and microglia (n = 4) to have at least three distinct isoforms, however, both had differential expression of each (Figures 4B and 4C). It was found that the most abundant isoform expressed within microglia was the 50 kDa isoform, while OPCs were found to predominantly have the 45 kDa isoform. Total protein quantification of all CXCR4 isoforms was found not to be significantly different between microglia (1.72 ± 0.31 a.u.) versus OPCs (1.33 ± 0.35 a.u.). CXCR7 expression was only barely detectable by western blot and not immunocytochemistry on both OPCs and microglia (Figure 4B). Therefore the pro-myelinating capabilities of CXCL12 could be mediated via its action on OPCs or microglia, or both. Purified OPCs were treated with CXCL12, OM-, or BM-MSC-CM (from three different patient samples for both) and labeled with markers of OPC differentiation (n = 3; Figure 4D). There were no differences in immunoreactivity of NG2 (early OPC marker), O4 (middle/late OPC marker), or PLP (late myelinating OPC marker). However, CXCL12 significantly changed OPC morphological appearance from a predominantly simple (bipolar) to a more complex (multi-branched) morphology, similar to that found with OM- or BM-MSC-CM treatment (Figure 4E; $p < 0.001$). OM-MSC-CM resulted in significantly more OPCs exhibiting a membranous morphology when compared with either control or BM-MSC-CM ($p < 0.001$ for both), and although the result of OM-MSC-CM treatment looked to be greater, it was not significantly different to CXCL12 treatment. Overall this suggests that CXCL12 can mediate morphological OPC differentiation via its direct action on the OPC itself. This hypothesis was confirmed by examining the effect of CXCL12, OM-, and BM-MSC-CM on purified OPCs incubated with inert nanofibers (Figure 4F). In these experiments, PLP-positive OPCs had significantly greater cell areas ensheathing axons in both CXCL12 and OM-MSC-CM compared with controls

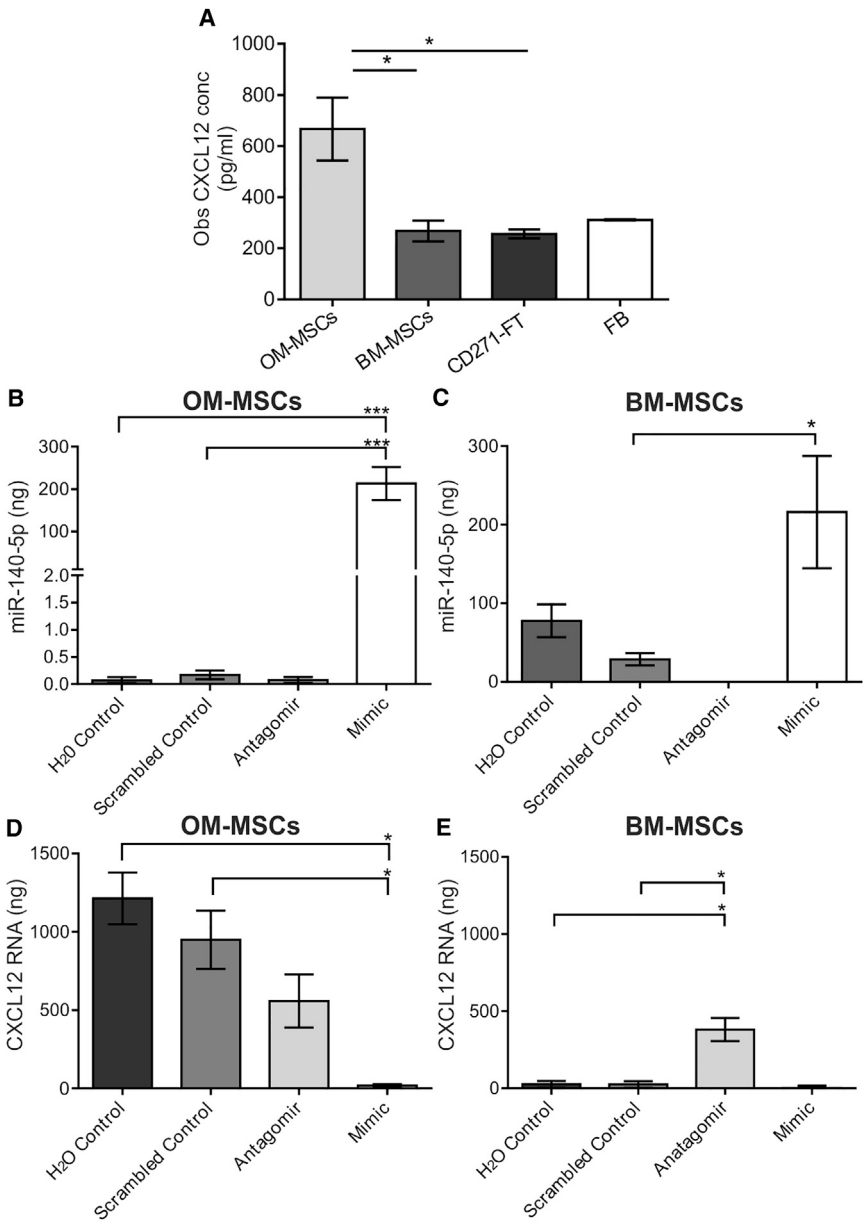

Figure 2. MiR-140-5p Regulates CXCL12 in OM-MSCs

(A) CXCL12 quantification in OM-MSC-CM, BM-MSC-CM, CD271-FT-CM, and fibroblast (FB)-CM. CXCL12 levels were significantly higher in OM-MSC-CM compared with all other cell types (n = 4 patient samples, mean ± SEM, *p < 0.05 determined by one-way ANOVA, Tukey's multiple comparison).

(B and C) qPCR analysis of OM- and BM-MSCs transfected with miR-140-5p antagomir or mimic, a scrambled control, and dH_2O only. MiR-140-5p expression was significantly greater in the mimic compared with controls (n = 3 patient samples, mean ± SEM, ***p < 0.001, one-way ANOVA, Tukey's multiple comparison). BM-MSCs transfected with the mimic significantly increased levels from control (n = 3 patient samples, mean ± SEM, *p < 0.05, one-way ANOVA, Tukey's multiple comparison).

(D) OM-MSC transfection with the miR-140-5p mimic caused significantly lower levels of CXCL12 mRNA compared with controls (n = 3 patient samples, mean ± SEM, *p < 0.05, one-way ANOVA, Tukey's multiple comparison).

(E) Antagomir induced a significant increase in CXCL12 mRNA in BM-MSCs compared with control levels (n = 3 patient samples, mean ± SEM, *p < 0.05, one-way ANOVA, Tukey's multiple comparison).

(n = 3 each treatment and patient samples). BM-MSC-CM also caused an increase in PLP-positive cell area, however this was found not to be significantly different from control due to the variability among samples (n = 3 patient samples). This suggests that both CXCL12 and OM-MSC-CM promoted process extension and wrapping in the absence of axonal signals to a greater extent than BM-MSC-CM.

Microglia are thought to polarize into distinct phenotypes, pro-inflammatory (depicted by iNOS expression) or anti-inflammatory (increased arginase I expression). To determine if the microglia phenotype plays a role in mediating myelination, we treated purified microglia with OM-, BM-MSC-CM (n = 4 patient samples for both), or CXCL12 (n = 4). CM from both cell types were tested for endogenous endotoxin levels (Pierce Endotoxin Quantification Kit; Thermo Scientific) to rule out any difference as a result of CM contamination prior to use. Lipopolysaccharide (LPS) and IL-4 were used as controls to induce the pro- and anti-inflammatory phenotype, respectively (Figures 4G and 4H). LPS stimulation shifted microglia predominantly to the pro-inflammatory phenotype assessed by increased iNOS expression compared with control (n = 4, $p < 0.01$), while IL-4-treated microglia expressed arginase I with no iNOS detectable (n = 4), suggesting a population that is similar to control. Treatment of microglia with OM-MSC-CM and CXCL12 increased arginase I expression compared

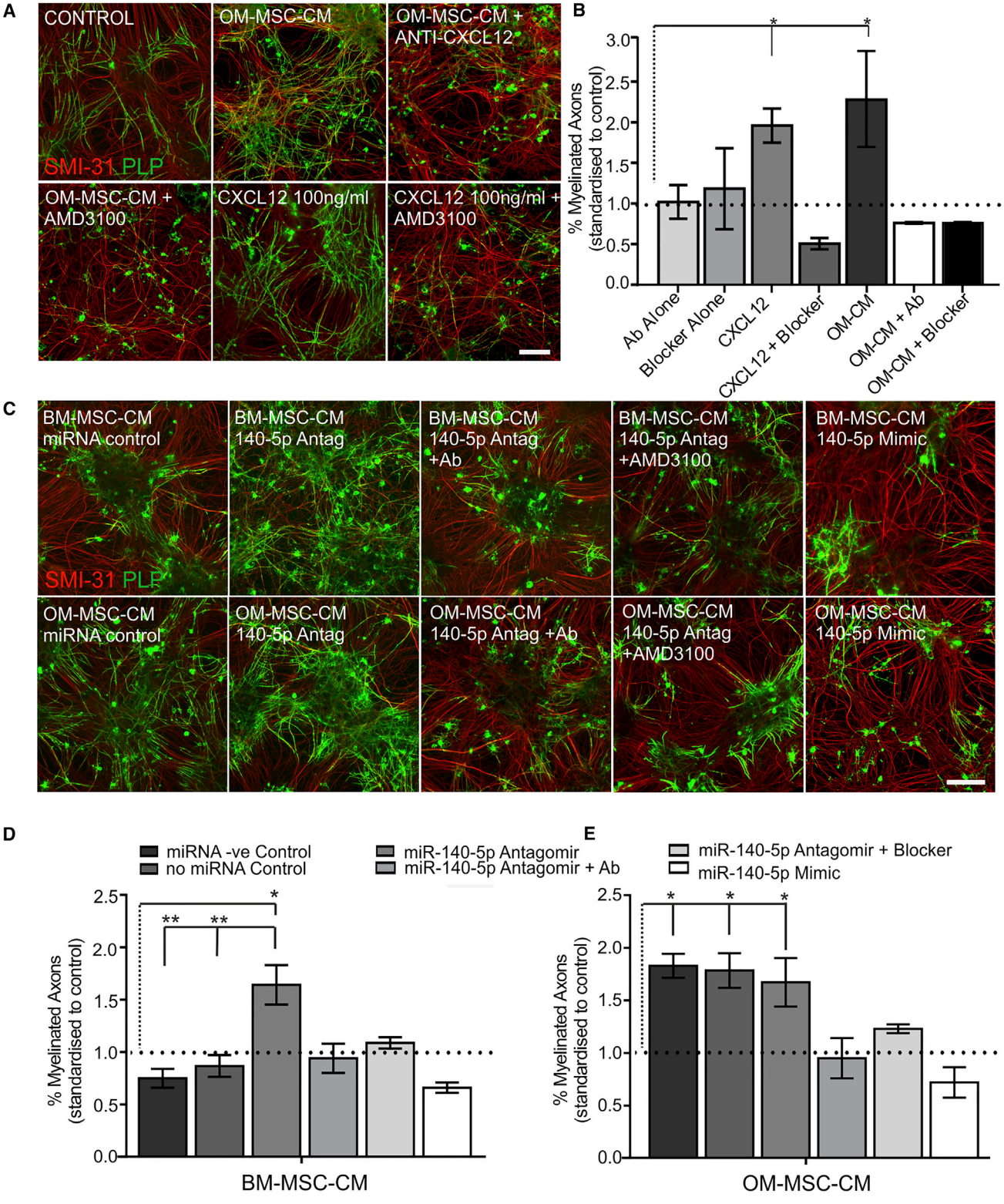

Figure 3. CXCL12 Promotes In Vitro CNS Myelination which is Regulated by miR-140-5p

(A) Co-cultures stained for myelin (green PLP) and axons (red SMI-31) treated with OM-MSC-CM, OM-MSC-CM in the presence of antibody to CXCL12 (OM-MSC-CM + anti-CXCL12), or CXCR4 blocker (OM-MSC-CM + AMD3100), CXCL12 (100 ng/ml), or CXCL12 in the presence of AMD3100. Scale bar represents 100 μm.

(legend continued on next page)

with the control ($p < 0.001$ and $p < 0.05$, respectively) with no detectable iNOS expression, suggesting a larger shift to the anti-inflammatory phenotype in both conditions. BM-MSC-CM did not stimulate a significant increase in arginase I levels from control but did however lead to increased iNOS production ($p < 0.01$), the only treatment besides LPS to do so (Figures 4G and 4H). This would strongly suggest that OM-MSC-CM and CXCL12 cause microglia to polarize predominantly to an anti-inflammatory phenotype, in contrast to BM-MSC-CM, which appears to shift them more toward a pro-inflammatory phenotype. Recently, the anti-inflammatory phenotype of microglia has been reported to play a role in myelination through the production of activin A (Miron et al., 2013). Therefore we assessed activin A levels within the CM of microglia treated with CXCL12 (n = 3) or OM- or BM-MSC-CM (n = 3 patient samples for both) with their respective CM used as controls (Figure 4I). It was found that there were no identifiable increases in activin A in CXCL12-treated cultures, and although OM- and BM-MSC-CM showed increased levels, this was similar to that already present within the CM alone. Therefore, both types of MSC, but not microglia, secrete activin A.

MiR-146a-5p Network and Chemokine Regulation

The GeneGo MetaCore network for miR-146a-5p indicated an association with Toll-like receptor (TLR) expression and the regulation of inflammatory chemokines. This suggests differential modulation of the inflammatory response, which is an important consideration for cell transplant-mediated repair. Total TLR2 and 4 levels were significantly less in OM-MSCs compared with BM-MSCs (n = 6 patient samples for both, $p < 0.01$ and $p < 0.05$, respectively; Figure 5A). There was notably less TLR2 expression in both cell types compared with their TLR4 expression since only TLR4 was present abundantly enough to be detected via fluorescence-activated cell sorting (FACS) (n = 3 patient samples for both; Figure 5B). MiR-146a-5p is thought to modulate the secretion of IL-6 and IL-8, and BM-MSC-CM was found to contain at least 1.5-fold more of both these and CCL2 than OM-MSC-CM (Figure 5C). Quantification was carried out by ELISA (n = 3 patient samples for both, $p < 0.01$, $p < 0.001$, and $p < 0.05$; Figure 5D).

The miR-146a-5p antagomir (Figure 6A) caused a significant reduction in miR-146a-5p miRNA levels in OM-MSCs ($p < 0.05$), however BM-MSCs, which have less of this miRNA constitutively, showed a non-significant reduction (n = 3, patient samples for both). The levels of IL-8, IL-6, and CCL2 were all assessed before and after LPS stimulation for 24 hr in CM collected from BM-MSCs, OM-MSCs, OM-MSC transfected with dH_2O or with a scrambled control, or with the miR-146-5p antagomir (n = 4 all treatments and n = 4 patient samples for both; Figures 6B–6D). Both control transfections expressed similar non-significant levels of cytokine expression before and after stimulation with LPS, therefore only dH_2O-transfected OM-MSC control data are presented. The higher secretion of IL-8, IL-6, and CCL2 within BM-MSC-CM in basal conditions compared with OM-MSC-CM was confirmed ($p < 0.05$, $p < 0.01$, $p < 0.05$, respectively). LPS caused IL-8 to increase to equivalent levels within OM-MSC-CM and BM-MSC-CM. However, OM-MSCs in the presence of the miR-146a-5p antagomir produced a significantly larger increase in LPS-stimulated IL-8 levels ($p < 0.05$), suggesting that repression of miR-146a-5p led to increased production of IL-8. IL-6 levels were found to be lower in OM-MSC-CM both before and after LPS stimulation when compared with BM-MSC-CM ($p < 0.01$ and $p < 0.001$, respectively). Transfection with miR-146a-5p antagomir caused an increase in the LPS-induced levels of IL-6 in OM-MSCs ($p < 0.05$). CCL2 levels, although lower in OM-MSCs compared with BM-MSCs under basal conditions ($p < 0.05$), was found not to be significantly different after LPS stimulation in antagomir-treated OM-MSCs (Figure 6D). These data provide evidence that miR-146-5p can regulate the secretion of both IL-6 and IL-8 but not CCL2 in both OM- and BM-MSCs.

(B) CXCL12 and OM-MSC-CM increased myelination significantly compared with control levels (demarcated by the dotted line). AMD3100 blocker and anti-CXCL12 abolished the pro-myelinating effect of OM-MSC-CM and CXCL12 but did not affect myelination on their own (n = 4 patient samples, mean ± SEM, *p < 0.05, one-way ANOVA, Tukey's multiple comparison).

(C) Representative images of co-cultures stained for myelin (green PLP) and axons (red SMI-31) treated with CM from BM- or OM-MSCs transfected with miRNA control, antagomir (140-5p Antag), or miR-140-5p mimic and miR-140-5p antagomir-derived CM in the presence of anti-CXCL12 (140-5p + Ab) or the blocker (140-5p + AMD3100). Scale bar represents 100 μm.

(D) CM from BM-MSCs treated with miR-140-5p antagomir led to a significant increase in myelination compared with control (n = 6 patient samples for all). The antagomir-induced increase could be reduced to control levels in the presence of anti-CXCL12 or AMD3100 blocker (n = 3 patient samples for both). CM from BM-MSCs induced by the miR-140-5p mimic also did not promote myelination.

(E) OM-MSC-CM collected after miR-140-5p mimic transfection significantly reduced the pro-myelinating effect of OM-MSCs while transfection with antagomir had no effect (n = 3 patient samples). In (D) and (E), mean ± SEM, *p < 0.05, **p < 0.01, one-way ANOVA, Tukey's multiple comparison.

Dotted horizontal lines demarcate control levels, vertical dotted lines detail experimental comparisons made to control.

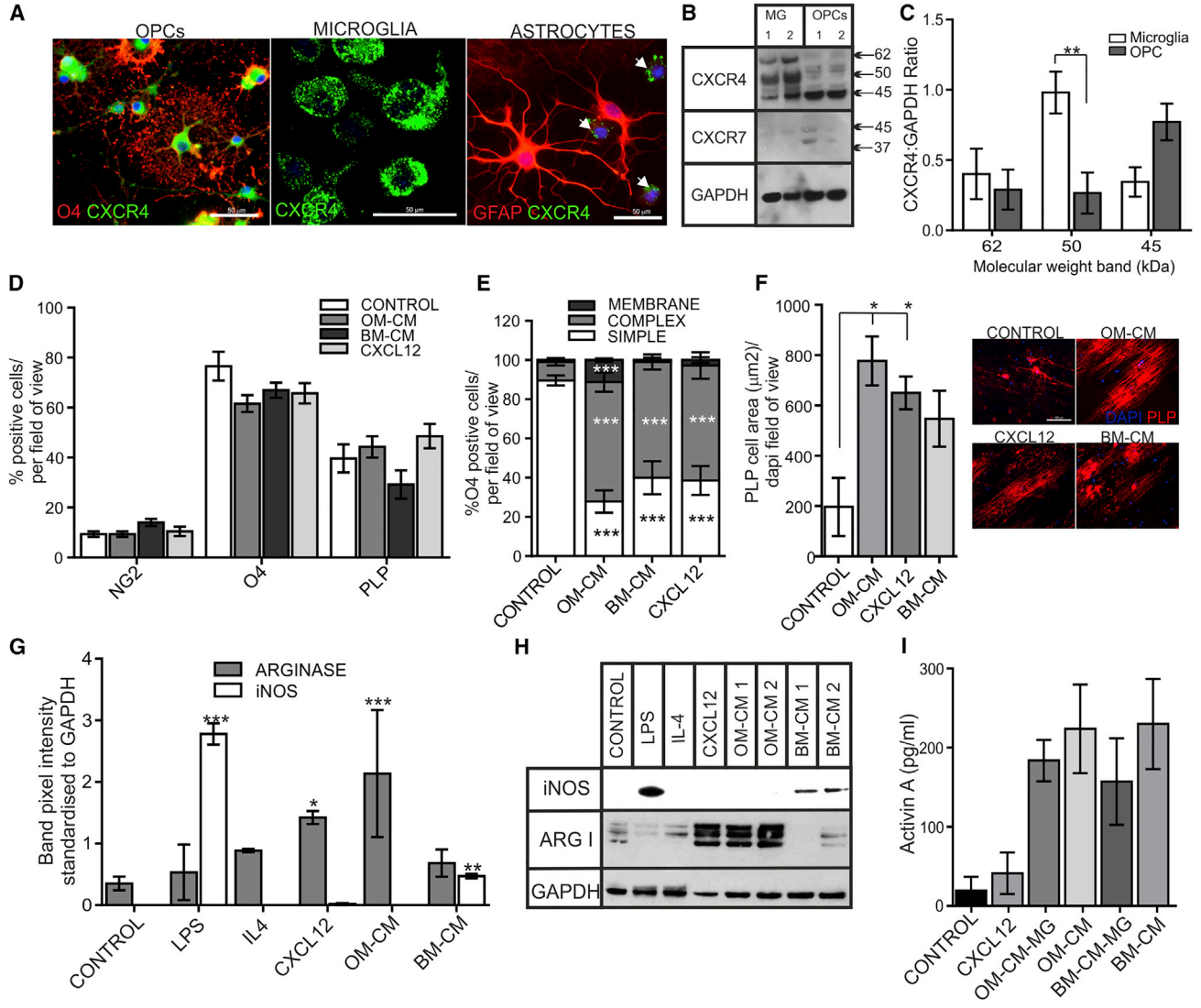

Figure 4. CXCL12 Action May Be via OPC Process Extension and Microglial Polarization

(A) CXCR4 expression (green) in oligodendrocytes (OPCs, red O4), microglia (MG) and astrocytes (GFAP, red). White arrows show microglia positive for CXCR4. Scale bar represents 50 µm.

(B) CXCR4 and CXCR7 protein levels in microglia (MG) and OPCs (n = 2, both cell types). GAPDH used as loading control.

(C) Graphical representation of western blot analysis. Microglia and OPCs show differing expression of various CXCR4 kDa bands. MG preferentially express the 50 kDa band (n = 4), while OPCs predominantly express the 45 kDa band (n = 6) (mean ± SEM, $^{**}p < 0.05$, two-way ANOVA, Sidak's multiple comparison).

(D) OPC differentiation was quantified using markers for OPCs (NG2), oligodendrocytes (O4), and mature oligodendrocytes (PLP) after CXCL12 treatment (n = 3), and CM from OM-MSCs (n = 3 patient samples) and BM-MSCs (n = 3 patient samples) compared with control (n = 3, mean ± SEM). No difference in marker expression was found.

(E) Process extension of OPCs assessed by O4. OM-MSC-CM (OM-CM, n = 3 patient samples), BM-MSC-CM (BM-CM, n = 3 patient samples), and CXCL12 treatment (n = 3) significantly increased the number of complex processes and reduced the number of simple processes formed compared with control media. OM-MSC-CM caused a significant increase in membranous process formation (mean ± SEM, $^{***}p < 0.001$, two-way ANOVA, Tukey's multiple comparison).

(F) Quantification of the PLP-positive cell area of OPCs grown on inert nanofibers and treated with OM-MSC-CM (n = 3, patient samples), BM-MSC-CM (n = 3, patient samples), or CXCL12 (n = 3). There was a significantly greater cell area in the presence of OM-CM and CXCL12 (mean ± SEM, $^{*}p < 0.05$ one-way ANOVA, Tukey multiple comparisons). Example images of OPCs (red PLP, blue DAPI) incubated with inert nanofibers. Scale bar represents 100 µm.

(legend continued on next page)

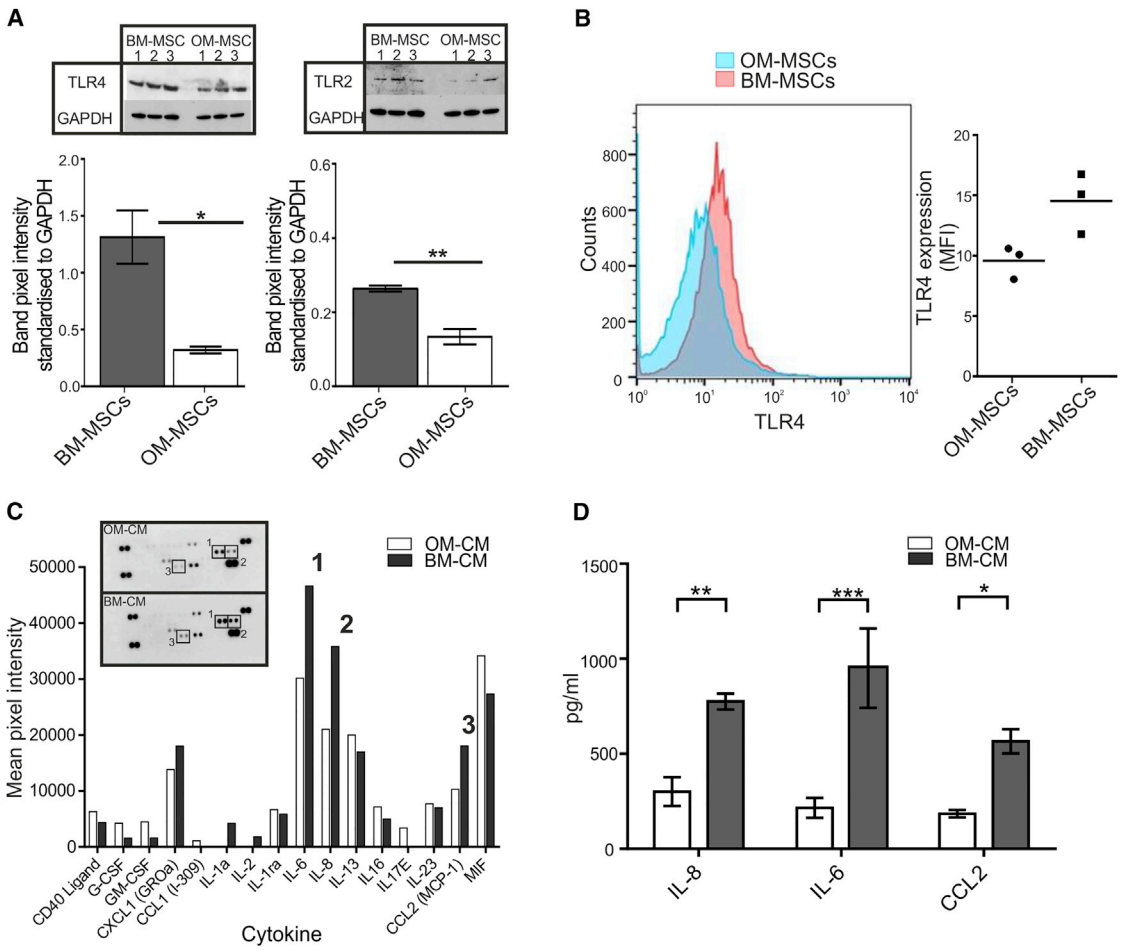

Figure 5. MiR-146-5p Differentially Regulates TLR4, TLR2, and Cytokine Secretion

(A) Graphical representation of TLR4 and TLR2 (western blot shown as inserts) in BM-MSCs (n = 6 patient samples) and OM-MSCs (n = 6 patient samples). BM-MSCs have significantly higher levels compared with OM-MSCs (mean ± SEM, *p < 0.05, **p < 0.01, Students unpaired t test).

(B) FACS analysis of TLR4 expression on OM- and BM-MSCs (n = 3, patient samples both).

(C) OM-MSC (n = 1 patient sample) and BM-MSC (n = 1 patient sample) cytokine profile. Insert shows dot plot while the graph illustrates the mean pixel intensity of the blot. IL-6 (1) IL-8 (2), and CCL2 (3) were expressed 1.5-fold higher in BM-MSC-CM.

(D) ELISA analysis of IL-8, IL-6, and CCL2 in BM-MSC-CM (n = 3 patient samples) and OM-MSC-CM (n = 3 patient samples, mean ± SEM, *p < 0.05, **p < 0.01, ***p < 0.001, Students unpaired t test).

DISCUSSION

In this investigation, miRNA-based fingerprinting demonstrated that OM- and BM-MSCs were 64% homologous, suggesting they have related regulatory miRNA patterns. Others have shown that MSCs derived from different tissue niches share expression of a core set of miRNAs that regulate associated target genes, although miRNA similarity

(G and H) Graphical representation of western blot analysis (H) of arginase I and iNOS after treatment with CXCL12 (n = 4), CM from OM-MSCs (n = 4 patient samples) and BM-MSCs (n = 4 patient samples), LPS (n = 4), IL-4 (n = 4), and control treatments (n = 4). iNOS was significantly upregulated in LPS and BM-MSC-CM (BM-CM) treatment. Arginase I levels were significantly upregulated in both CXCL12 and OM-MSC-CM (OM-CM) (mean ± SEM *p < 0.05, **p < 0.01, ***p < 0.001, one-way ANOVA, Tukey's multiple comparison).

(I) Quantification of activin A in microglia media after stimulation with CXCL12 (n = 3), OM-MSC-CM (OM-CM-MG, n = 3 patient samples) and BM-MSC-CM (BM-MSC-MG, n = 3 patient samples) for 24 hr. OM-MSC-CM (OM-CM) and BM-MSC-CM (BM-CM) were used as controls (mean ± SEM).

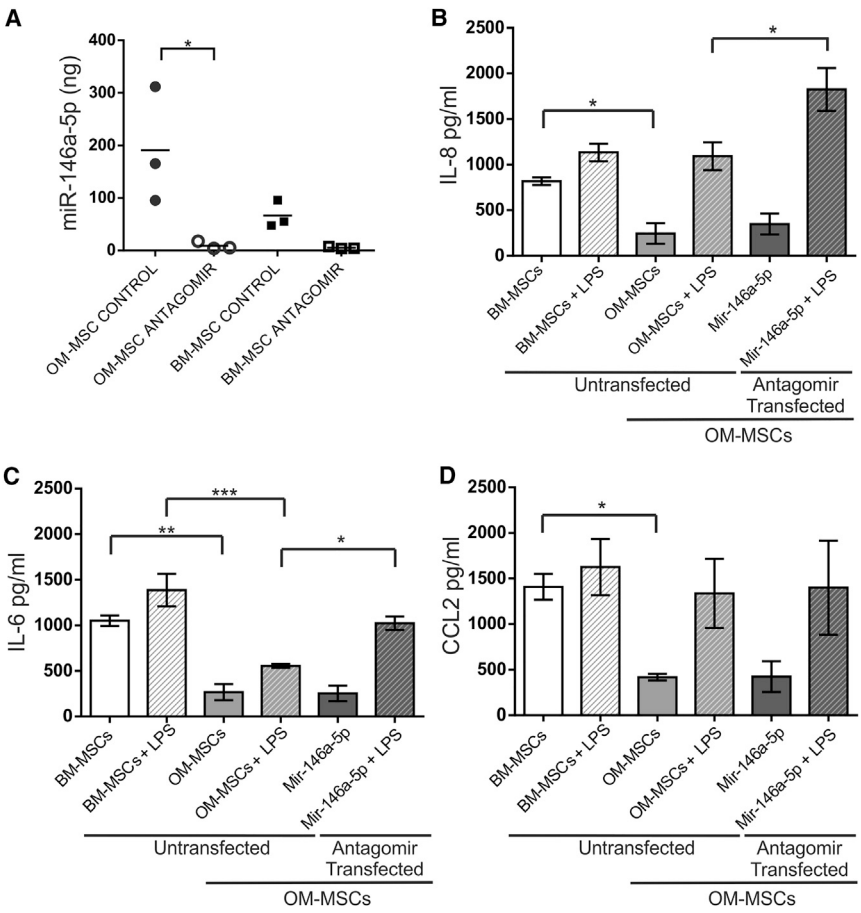

Figure 6. Regulation of IL-6 and IL-8 by miR-146a-5p

(A) qPCR of miR-146a-5p levels in OM-MSCs (n = 3 patient samples) and BM-MSCs (n = 3 patient samples) after transduction with antagomir. There was a significant reduction within OM-MSCs (mean ± SEM, *p < 0.05, one-way ANOVA with Tukey's multiple comparison).

(B–D) Quantification of IL-8 (B), IL-6 (C), and CCL2 (D) in OM-MSC-CM (OM-MSCs, n = 4 patient samples) and BM-MSC-CM (BM-MSCs, n = 4 patient samples) before and after LPS treatment (Untransfected), and OM-MSCs after transfection with the antagomir to miR-146a-5p (Antagomir Transfected). (B) OM-MSCs secrete less IL-8 compared with BM-MSCs. LPS stimulation of OM-MSCs caused an increase in IL-8 levels, which was significantly greater in the presence of the antagomir (mean ± SEM, *p < 0.05, one-way ANOVA, Tukey's multiple comparison). (C) IL-6 levels were significantly less in OM-MSCs compared with BM-MSCs both before and after LPS stimulation. IL-6 could be induced by LPS to greater levels in the presence of the antagomir (mean ± SEM, *p < 0.05, **p < 0.01, ***p<0.001, one-way ANOVA, Tukey's multiple comparison). (D) CCL2 was secreted significantly less in OM-MSC-CM compared with BM-MSC-CM. There were no differences before or after LPS stimulation or in the presence of the antagomir (mean ± SEM, *p < 0.05, one-way ANOVA, Tukey's multiple comparison).

between the two MSC types here was greater than that reported for other MSCs (Lazzarini et al., 2014). We identified 26 DE miRNAs, which could explain their different biological properties. We focused on miRNAs associated with chemokine production and myelination. and therefore examined miR-146a-5p, and miR-140-5p in more detail due to their reported association (Nicolas et al., 2008; Suzuki et al., 2010; Göttle et al., 2010; Hsieh et al., 2013).

MiR-140-5p (downregulated in OM-MSCs) has been reported to inhibit the expression of CXCL12 (Nicolas et al., 2008), which has been shown to promote oligodendroglial cell maturation in vitro (Göttle et al., 2010; Kadi et al., 2006) and myelination in the demyelinated cuprizone model (Patel et al., 2012). Given that miR-140-5p is downregulated in OM-MSCs, it was possible that *CXCL12* expression correlated with their increased myelinating capabilities. We demonstrated that OM-MSCs secreted significantly greater amounts of CXCL12, confirmed its pro-myelinating effect using myelinating co-cultures, and using miR-140-5p mimic/antagomir, we demonstrated an inverse relationship of mRNA for secreted *CXCL12*. Moreover, CM from MSCs transduced with the miR-140-5p antagomir and mimic affected CNS myelination in vitro, indicating that the pro-myelinating effect of OM-MSCs was due, at least in part, to CXCL12 secretion controlled by miR-140-5p. This reveals an important role for MSC-secreted CXCL12 in myelination. It is well understood that CXCL12 is vital in controlling hematopoietic stem cell and progenitor function within the human and rodent BM (Isern et al., 2014; Greenbaum et al., 2013) and that there are certain cell types that secrete high levels of CXCL12: CXCL12-abundant reticular (CAR) cells, nestin-GFP + stromal cells, and leptin receptor + stromal cells. However, what is not known currently is whether CD271 selection isolates which cell population from the BM, although a recent report has demonstrated nestin gene expression after CD271 purification (Li et al., 2014). Since we have previously shown our BM-MSCs to be only 50% nestin positive, it would suggest we are harvesting only some of the nestin-positive cells previously shown to

secrete CXCL12 (Isern et al., 2014; Greenbaum et al., 2013). CD271 may also isolate a population that does not produce CXCL12 or produces it in only low amounts, unlike in the OM where it exclusively isolates the nestin-positive MSCs. However, a direct correlation between nestin, CD271 expression, and CXCL12 secretion has yet to be established in OM-MSCs.

To elucidate CXCL12 mechanism of action, we determined the cellular expression of its receptors (Lipfert et al., 2013). Both OPCs and microglia strongly expressed multiple isoforms of CXCR4, which may reflect various post-transcriptional modifications that have been shown to exist previously (Sloane et al., 2005; Carlisle et al., 2009). CXCR7 expression could be detected only weakly, suggesting that the predominant receptor type is CXCR4. OPCs responded to CXCL12 by enhanced process branching and membrane formation, however myelin marker differentiation remained unchanged. Since a prominent activity for chemokines is to regulate leukocyte trafficking, which is considered to occur through actin cytoskeleton modulation (Thelen and Stein, 2008), it could be that CXCL12 regulates OPC actin cytoskeleton during process extension in myelination.

Since microglia express CXCR4, it is possible that CXCL12 may indirectly influence myelination through their activity. Microglia are both a source and/or target for CXCL12 (Albright et al., 1999; Lee et al., 2002), which promotes their migration and proliferation. Microglia treated with CXCL12 or OM-, not BM-MSC-CM, upregulated arginase I expression, which resembles polarization seen in anti-inflammatory macrophages (Murray et al., 2014). Conversely, iNOS expression was induced by BM-MSC-CM but not CXCL12 or OM-MSC-CM. These differences suggest that OM-MSCs induce microglia to polarize predominantly to a more anti-inflammatory phenotype, in contrast to BM-MSC-CM, which appears to shift them toward a pro-inflammatory phenotype. Although the anti-inflammatory phenotype is thought to play a role in myelination via activin A (Miron et al., 2013), there was no difference in activin A levels in CM of both MSCs or an upregulation of it in treated microglia, suggesting that this is not the mechanism.

Further studies were carried out on miR-146a-5p, which is thought to be a mediator of inflammation, and a regulator of IL-6 and IL-8 and the expression of the immune receptors TLR2 and 4 (Taganov et al., 2006). TLRs are present on a range of non-immune cells, and a number (predominantly TLR2 and TLR4) can be stimulated by endogenous ligands termed damage-associated molecular patterns. Hence the role they play in the pathophysiology of cell transplantation is important (Leventhal and Schröppel, 2012). Stimulation of TLRs on MSCs by endogenous ligands released during inflammation and cellular stress has been linked to the perpetuation of chronic inflammatory responses after transplantation (DelaRosa and Lombardo, 2010). Therefore, one could postulate that transplanted cells that have fewer TLRs present would induce a lower inflammatory response.

The pro-inflammatory cytokines IL-6, IL-8, and CCL2 were constitutively secreted in greater levels in BM-MSC-CM compared with OM-MSC-CM, although LPS-treated OM-MSCs only had reduced levels of IL-6. Since LPS stimulation in the presence of miR-146a-5p antagomir resulted in significantly greater levels of IL-6 and IL-8 secreted by OM-MSCs, this corroborates the inhibitory role of miR-146a-5p in regulating their secretion. It should be noted, however, that the levels were not higher than those constitutively secreted by BM-MSCs. So while miR-146a-5p antagomir transfection has shown modest effects after LPS stimulation, it may not be enough to upregulate the secretion of IL-6 and IL-8 to high levels. This is presumably since these two cytokines are predicted to be targeted by 18 and 30 other miRNAs, respectively, which may have a regulatory role. CCL2, which is not thought to be on the same miR-axis, was not upregulated with antagomir treatment, suggesting that this miRNA was specific for the regulation of IL-6 and IL-8. Moreover, it is tempting to speculate that the induction of the pro-inflammatory phenotype of microglia by BM-MSC-CM is due to their differing cytokine secretion.

With increasing evidence that nestin-positive MSCs that reside in the bone marrow are from the neural crest and a subpopulation that secrete CXCL12 (Isern et al., 2014), it is possible that OM-MSCs are an enriched population of these neural-crest-derived MSCs. Equally, as BM-MSCs are a heterogeneous population, it is plausible that purifying the nestin-positive cells may result in enhancing their CNS repair potential to similar levels as OM-MSCs. Given our findings and that OM-MSCs are an easily accessible source of cells; we propose that they may be an alternative cellular source for cell-transplant-mediated CNS repair.

EXPERIMENTAL PROCEDURES

Cell Culture

Culture of Human Olfactory Mucosa MSCs

Biopsy samples were obtained with Central Office for Research Ethics Committees (COREC, REC reference 07/S0710/24) ethical approval and informed patient consent from the upper middle turbinates in 21 patients undergoing nasal septoplasty surgery, aged between 26 and 93 years (average age, 55.0 ± 3.4 years; Table S1). They were purified using CD271 (Quirici et al., 2002) and grown as previously described (Lindsay et al., 2013). Purification using CD271 selection allows MSCs to be specifically selected from fibroblasts and other adherent populations. Before use, cells were assessed for MSC surface antigens and myelinating potential as

described previously (Lindsay et al., 2013). Purified cells were termed OM-MSCs while flow-through (FT) cells were retained and termed CD271-negative FT cells (CD271-FT). FT cells do not bind CD271 and are thus a contaminating cell population. CD271-FT were used to ensure secreted factors were specifically generated from the purified MSCs.

Culture of Human Bone Marrow MSCs

BM aspirates were obtained with ethical approval and informed patient consent from iliac crests of 18 patients undergoing hip replacement aged 33 to 86 years (average age, 63.9 ± 3.1 years; Table S1). BM collected in DMEM containing 5% fetal bovine serum (FBS), 0.5% heparin, 0.1% EDTA was layered onto Histopaque-1077 then centrifuged at 400 × *g*. After washes (PBS, 5% FBS, and 0.1% EDTA), the pellet was resuspended in 10% αMEM and plated on collagen-coated (10 μg/ml; Sigma-Aldrich) 25 cm^2 tissue culture flasks. MSCs were isolated by standard plastic adherence and, upon confluency, were purified similar to OM-MSCs using the EasySep Human MSC CD271 Positive Selection Kit (STEMCELL Technologies) so that direct comparisons could be made. Cells were assessed for expression of MSC surface antigens and myelinating potential prior to use (Lindsay et al., 2013).

Collection of Conditioned Media

CM was collected from flasks of different donor patients of OM-MSCs, BM-MSCs, CD271-FT, or human dermal fibroblasts (HDF; Supplemental Experimental Procedures) at P2-P4. For OPC, microglia, and chemokine experiments, CM was collected in DMEM modified by Bottenstein and Sato (1979) (DMEM-BS). For myelinating culture experiments, CM was collected in DM (Lindsay et al., 2013). After 72 hr, the CM was collected and used immediately or stored at −20°C. Cell counts after collection ensured no significant differences in cell number between flasks.

Culture of Rat Microglia and Oligodendrocyte Precursor Cells

Sprague Dawley cortices were digested and grown in DMEM containing 10% FBS with 4.5 g/l glucose, L-glutamine, pyruvate, and 1% penicillin/streptomycin (DMEM-10%) using standard methods (Noble and Murray, 1984). After 7–10 days, microglia and OPCs were purified by differential attachment (Miron et al., 2013). See Supplemental Experimental Procedures for details.

Myelinating Spinal Cord Rat Cultures

Myelinating spinal cord co-cultures were set up using standard methods (Sørensen et al., 2008). After 12 days, insulin was withdrawn and cultures treated until day 28 by the addition of OM- or BM-MSC-CM diluted 1:2 with DM, CXCL12 (100 ng/ml; Peprotech), anti-CXCL12 (10 μg/ml; R&D Systems), and CXCR4 antagonist, AMD3100 (50 μM; Sigma). AMD3100 was added for 1 hr prior to feeding to allow binding. In antagomir/mimic experiments, CM from transfected BM- or OM-MSCs was added at day 12 or pre-treated with anti-CXCL12 before addition. Information on quantification of myelination can be found in Supplemental Experimental Procedures.

Microarray Analysis

RNA Isolation

RNA from four donors of OM-MSCs (n = 4) and BM-MSCs (n = 4) grown to P4 was prepared using an Exiqon miRCURY RNA Kit. Absorbance ratios were determined as indicators of sample yield and purity. RNA quality control was performed using the Agilent 2100 Bioanalyser and the RNA 6000 Nano Kit according to the manufacturer's instructions, to determine the RNA integrity number. Samples were analyzed on the Agilent miRNA platform (Agilent's SurePrint G3 Human v16 microRNA 8 × 60K microarray slides; miRBase version 16.0). 100 ng of RNA was used as input for each microarray.

Microarray

Eight individual microarrays, representing 1,349 miRNAs, 1,205 human (1,199 verified as real miRNAs in miRbase 18), and 144 viral were used. The accession number for the microarray reported in this paper is ArrayExpress: E-MTAB-4594. Methods are found in Supplemental Experimental Procedures.

Antagomir, Mimic, and miRNA Transfection

BM- and OM-MSCs were transfected using Attractene Fast-Forward (Qiagen). Twelve-well plates were seeded with 1 × 10^5 cells/well and 50 nM mirVana miRNA miR-140-5p inhibitor (Ambion, MH10205) and mimic (MC10205), mi-146a-5p inhibitor (MH10722) and mimic (MC10205), miRNA negative (scrambled) control (RNU58A) or dH_2O (no miRNA control) was added in triplicate. Plates were incubated at 37°C for 24 hr, then cells were lysed for mRNA, or the media replaced with DM for 48 hr for CM collection, which was used to treat myelinating cultures.

qPCR

RNA content was analyzed using Nanondrop 1000 (Thermo Scientific) and cDNA synthesized using QuantiTect reverse transcription (Qiagen). qRT-PCR was performed using SYBR MasterMix (Qiagen) by StepOnePlus Real-Time PCR (Applied Biosystems) in triplicate. Log C_T values were calculated and plotted against concentration to produce a standard curve from which each sample was extrapolated. For primers, see Supplemental Experimental Procedures.

Chemokine Assays

Multiplex Cytokine/Chemokine Assay

CM from BM-, OM-MSCs, HDF, and CD271-FT (n = 4, in triplicate) were analyzed using Milliplex human cytokine/chemokine magnetic 23 bead panel II (Millipore; HCP2MAG-62K-PX23) run on the Bio-Rad Bio-Plex with Luminex 200 and Human Chemokine Array Kit (Invitrogen; LHC6003) following the manufacturer's protocol.

ELISA

IL-8, IL-6, and CCL2 ELISA MAX Deluxe kits (Biolegend) were used according to the manufacturer's protocol to assess OM- and BM-MSC-CM before and after overnight LPS stimulation (10 ng/ml; Sigma) or after miR-140-5p antagomir transduction as previously described. Both the Human Multi-Neurotrophin Rapid Screening ELISA Kit (Biosensis) and Human Activin A Kit (BD Bioscience) were used as per the manufacturers' protocols. All ELISA samples were run in triplicate.

Western Blot

Cells were lysed using CelLytic M (Sigma) containing protease inhibitor cocktail (Sigma) and protein concentration determined (NanoDrop; Thermo Scientific). Samples were run using standard methods described in Supplemental Experimental Procedures.

FACS Analysis

OM- and BM-MSCs were incubated with human receptor FC block (eBioscience; 14-9161-71) for 20 min, followed by TLR4-488 (eBioscience; 53-9917-41) or mouse isotype control 488 (eBioscience; 53-4724-80) for 20 min on ice. Cells were washed then resuspended in PBS containing 2% paraformaldehyde and evaluated by flow cytometry in an FACS Caliber (BD) and analyzed using FlowJo.

Statistical Analysis

For each independent experiment, data were collected using MSCs generated from at least three different patients. Donor-derived cells were used up to passage four, limiting the number of experiments that could be conducted from individual samples; thus multiple MSC donors were required to complete all experiments. Table S2 details which biopsies were used for each experiment. Data are presented as the mean ± SEM and analyzed using Student's t test, ANOVA with Dunnett post-test, Sidak's or Tukey's adjustment for multiple comparisons where appropriate, using Prism software version 5.0 (GraphPad Software). Differences were considered significant at $p < 0.05$.

SUPPLEMENTAL INFORMATION

Supplemental Information includes Supplemental Experimental Procedures and two tables and can be found with this article online at http://dx.doi.org/10.1016/j.stemcr.2016.03.009.

AUTHORS CONTRIBUTIONS

Conception and Design: S.L.L., S.C.B., S.A.J., and D.M.; Preliminary Work: M.A.McG.; Interpreted Data: S.L.L., S.A.J., D.M., and M.A.McG.; Writing – Original Draft: S.L.L. and S.C.B.; Writing – Review & Editing: S.C.B. and S.L.L.; Funding Acquisition: S.C.B.

ACKNOWLEDGMENTS

This work was funded by Tenovus Foundation (S.L.L.), Medical Research Council (MRC) (S.L.L., MR/J004731/1), Lord Kelvin/Adam Smith University of Glasgow (S.A.J.), and NC3Rs (M.A.McG., NC/K50032X/1). We thank Mr Allan, Mr Robertson, Miss Clark, Mr Meek (Southern General Hospital, Glasgow) and Mr Sheikh (Victoria Hospital, Glasgow) for generously providing human tissue.

Received: September 10, 2015
Revised: March 23, 2016
Accepted: March 24, 2016
Published: April 21, 2016

REFERENCES

Albright, A.V., Shieh, J.T., Itoh, T., Lee, B., Pleasure, D., O'Connor, M.J., Doms, R.W., and González-Scarano, F. (1999). Microglia express CCR5, CXCR4, and CCR3, but of these, CCR5 is the principal coreceptor for human immunodeficiency virus type 1 dementia isolates. J. Virol. *73*, 205–213.

Ambros, V. (2001). microRNAs: tiny regulators with great potential. Cell *107*, 823–826.

Bonab, M.M., Sahraian, M.A., Nikbin, B., Lotfi, J., Khorramnia, S., Motamed, M.R., Togha, M., Harirchian, M.H., Moghadam, N.B., Alikhani, K., et al. (2012). Autologous mesenchymal stem cell therapy in progressive multiple sclerosis: an open label study. Curr. Stem Cell. Res. Ther. *7*, 407–414.

Bottenstein, J.E., and Sato, G.H. (1979). Growth of a rat neuroblastoma cell line in serum-free supplemented medium. Proc. Natl. Acad. Sci. USA *76*, 514–517.

Carlisle, A.J., Lyttle, C.A., Carlisle, R.Y., and Maris, J.M. (2009). CXCR4 expression heterogeneity in neuroblastoma cells due to ligand-independent regulation. Mol. Cancer *8*, 126.

Collino, F., Bruno, S., Deregibus, M.C., Tetta, C., and Camussi, G. (2011). MicroRNAs and mesenchymal stem cells. Vitam. Horm. *87*, 291–320.

Connick, P., Kolappan, M., Crawley, C., Webber, D.J., Patani, R., Michell, A.W., Du, M.Q., Luan, S.L., Altmann, D.R., Thompson, A.J., et al. (2012). Autologous mesenchymal stem cells for the treatment of secondary progressive multiple sclerosis: an open-label phase 2a proof-of-concept study. Lancet Neurol. *11*, 150–156.

DelaRosa, O., and Lombardo, E. (2010). Modulation of adult mesenchymal stem cells activity by toll-like receptors: implications on therapeutic potential. Med. Inflamm. *2010*, 865601.

Gao, J., Yang, T., Han, J., Yan, K., Qiu, X., Zhou, Y., Fan, Q., and Ma, B. (2011). MicroRNA expression during osteogenic differentiation of human multipotent mesenchymal stromal cells from bone marrow. J. Cell Biochem. *112*, 1844–1856.

Göttle, P., Kremer, D., Jander, S., Odemis, V., Engele, J., Hartung, H.P., and Küry, P. (2010). Activation of CXCR7 receptor promotes oligodendroglial cell maturation. Ann. Neurol. *68*, 915–924.

Graziadei, P.P., and Monti Graziadei, G. (1985). Neurogenesis and plasticity of the olfactory sensory neurons. Ann. N. Y. Acad. Sci. *457*, 127–142.

Greenbaum, A., Hsu, Y.M., Day, R.B., Schuettpelz, L.G., Christopher, M.J., Borgerding, J.N., Nagasawa, T., and Link, D.C. (2013). CXCL12 in early mesenchymal progenitors is required for haematopoietic stem-cell maintenance. Nature *495*, 227–230.

Hass, R., Kasper, C., Böhm, S., and Jacobs, R. (2011). Different populations and sources of human mesenchymal stem cells (MSC): a comparison of adult and neonatal tissue-derived MSC. Cell Commun. Signal. *9*, 12.

Hsieh, J.Y., Huang, T.S., Cheng, S.M., Lin, W.S., Tsai, T.N., Lee, O.K., and Wang, H.W. (2013). miR-146a-5p circuitry uncouples cell proliferation and migration, but not differentiation, in human mesenchymal stem cells. Nucleic Acids Res. *41*, 9753–9763.

Isern, J., and Méndez-Ferrer, S. (2011). Stem cell interactions in a bone marrow niche. Curr. Osteoporos. Rep. *9*, 210–218.

Isern, J., García-García, A., Martín, A.M., Arranz, L., Martín-Pérez, D., Torroja, C., Sánchez-Cabo, F., and Méndez-Ferrer, S. (2014). The neural crest is a source of mesenchymal stem cells with specialized hematopoietic stem cell niche function. eLife *3*, e03696.

Johnstone, S.A., Liley, M., Dalby, M.J., and Barnett, S.C. (2015). Comparison of human olfactory and skeletal MSCs using osteogenic nanotopography to demonstrate bone-specific bioactivity of the surfaces. Acta Biomater. *13*, 266–276.

Kadi, L., Selvaraju, R., de Lys, P., Proudfoot, A.E., Wells, T.N., and Boschert, U. (2006). Differential effects of chemokines on oligodendrocyte precursor proliferation and myelin formation in vitro. J. Neuroimmunol. *174*, 133–146.

Lazzarini, R., Olivieri, F., Ferretti, C., Mattioli-Belmonte, M., Di Primio, R., and Orciani, M. (2014). mRNAs and miRNAs profiling of mesenchymal stem cells derived from amniotic fluid and skin: the double face of the coin. Cell Tissue Res. *355*, 121–130.

Lee, Y.B., Nagai, A., and Kim, S.U. (2002). Cytokines, chemokines, and cytokine receptors in human microglia. J. Neurosci. Res. *69*, 94–103.

Leventhal, J.S., and Schröppel, B. (2012). Toll-like receptors in transplantation: sensing and reacting to injury. Kidney Int. *81*, 826–832.

Li, H., Ghazanfari, R., Zacharaki, D., Ditzel, N., Isern, J., Ekblom, M., Méndez-Ferrer, S., Kassem, M., and Scheding, S. (2014). Low/negative expression of PDGFR-α identifies the candidate primary mesenchymal stromal cells in adult human bone marrow. Stem Cell Rep. *6*, 965–974.

Lindsay, S.L., Johnstone, S.A., Mountford, J.C., Sheikh, S., Allan, D.B., Clark, L., and Barnett, S.C. (2013). Human mesenchymal stem cells isolated from olfactory biopsies but not bone enhance CNS myelination in vitro. Glia *61*, 368–382.

Lipfert, J., Ödemis, V., Wagner, D.C., Boltze, J., and Engele, J. (2013). CXCR4 and CXCR7 form a functional receptor unit for SDF-1/CXCL12 in primary rodent microglia. Neuropathol. Appl. Neurobiol. *39*, 667–680.

Ma, X.L., Liu, K.D., Li, F.C., Jiang, X.M., Jiang, L., and Li, H.L. (2013). Human mesenchymal stem cells increases expression of a-tubulin and angiopoietin 1 and 2 in focal cerebral ischemia and reperfusion. Curr. Neurovasc. Res. *10*, 103–111.

Miron, V.E., Boyd, A., Zhao, J.W., Yuen, T.J., Ruckh, J.M., Shadrach, J.L., van Wijngaarden, P., Wagers, A.J., Williams, A., Franklin, R.J., et al. (2013). M2 microglia and macrophages drive oligodendrocyte differentiation during CNS remyelination. Nat. Neurosci. *16*, 1211–1218.

Murray, P.J., Allen, J.E., Biswas, S.K., Fisher, E.A., Gilroy, D.W., Goerdt, S., Gordon, S., Hamilton, J.A., Ivashkiv, L.B., Lawrence, T., et al. (2014). Macrophage activation and polarization: nomenclature and experimental guidelines. Immunity *17*, 14–20.

Nakano, N., Nakai, Y., Seo, T.B., Yamada, Y., Ohno, T., Yamanaka, A., Nagai, Y., Fukushima, M., Suzuki, Y., Nakatani, T., and Ide, C. (2010). Characterization of conditioned medium of cultured bone marrow stromal cells. Neurosci. Lett. *483*, 57–61.

Nicolas, F.E., Pais, H., Schwach, F., Lindow, M., Kauppinen, S., Moulton, V., and Dalmay, T. (2008). Experimental identification of microRNA-140 targets by silencing and overexpressing miR-140. RNA *14*, 2513–2520.

Noble, M., and Murray, K. (1984). Purified astrocytes promote the in vitro division of a bipotential glial progenitor cell. EMBO. J. *3*, 2243–2247.

Patel, J.R., Williams, J.L., Muccigrosso, M.M., Liu, L., Sun, T., Rubin, J.B., and Klein, R.S. (2012). Astrocyte TNFR2 is required for CXCL12-mediated regulation of oligodendrocyte progenitor proliferation and differentiation within the adult CNS. Acta Neuropathol. *124*, 847–860.

Quirici, N., Soligo, D., Bossolasco, P., Servida, F., Lumini, C., and Deliliers, G.L. (2002). Isolation of bone marrow mesenchymal stem cells by anti-nerve growth factor receptor antibodies. Exp. Hematol. *7*, 783–791.

Skalnikova, H., Motlik, J., Gadher, S.J., and Kovarova, H. (2011). Mapping of the secretome of primary isolates of mammalian cells, stem cells and derived cell lines. Proteomics *11*, 691–708.

Sloane, A.J., Raso, V., and Dimitrov, D.S. (2005). Marked structural and functional heterogeneity in CXCR4: separation of HIV-1 and SDF-1[alpha] responses. Immunol. Cell Biol. *83*, 129–143.

Sørensen, A., Moffat, K., Thomson, C., and Barnett, S.C. (2008). Astrocytes but not olfactory ensheathing cells or Schwann cells promote myelination of CNS axons in vitro. Glia *56*, 750–763.

Suzuki, Y., Kim, H.W., Ashraf, M., and Haider, H.K. (2010). Diazoxide potentiates mesenchymal stemcell survival via NF-kappaB-dependent miR-146a expression by targeting. Fas. Am. J. Physiol. Heart Circ. Physiol. *299*, H1077–H1082.

Taganov, K.D., Boldin, M.P., Chang, K.J., and Baltimore, D. (2006). NFkappaB-dependent induction of microRNA miR-146, an inhibitor targeted to signaling proteins of innate immune responses. Proc. Natl. Acad. Sci. USA *103*, 12481–12486.

Thelen, M., and Stein, J.V. (2008). How chemokines invite leukocytes to dance. Nat. Immunol. *9*, 953–959.

Tomé, M., Lopez-Romero, P., Albo, C., Sepulveda, J.C., Fernandez-Gutierrez, B., Dopazo, A., Bernad, A., and González, M.A. (2011). miR-335 orchestrates cell proliferation, migration and differentiation in human mesenchymal stem cells. Cell Death Differ. *18*, 985–995.

Tondreau, T., Lagneaux, L., Dejeneffe, M., Massy, M., Mortier, C., Delforge, A., and Bron, D. (2004). Bone, marrow-derived mesenchymal stem cells already express specific neural proteins before any differentiation. Differentiation *72*, 319–326.

Wang, X., Wang, Y., Gou, W., Lu, Q., Peng, J., and Lu, S. (2013). Role of mesenchymal stem cells in bone regeneration and fracture repair: a review. Int. Orthop. *37*, 2491–2498.

Wiese, C., Rolletschek, A., Kania, G., Rolletschek, A., Kania, G., Blyszczuk, P., Tarasov, K.V., Tarasova, Y., Wersto, R.P., Boheler, K.R., et al. (2004). Nestin expression-a property of multi-lineage progenitor cells? Cell Mol. Life Sci. *61*, 2510–2522.